

Discrete Differential Operators Immediately Applicable to Numerical Models of Solid Mechanics

A.A. Zisman*, N.Yu. Ermakova

Institute of Physics and Mechanics, Peter the Great St. Petersburg Polytechnic University, Politekhnickeskaya ul., 29, St. Petersburg 195251, Russia

Article history

Received September 17, 2022
Accepted September 20, 2022
Available online September 30, 2022

Abstract

The conventional gradient and related differential operators have been uniquely extended to a cluster of nodal points. Based on general algebraic grounds, such extensions are applicable to any discrete pattern while avoiding artificial shape functions or tessellations. Thus, various constitutive equations can be represented in a discrete form that enables the numerical modeling immediately in terms of nodal variables. Accuracy of this approach should ameliorate by the reduction of nodal spacing with the increasing computational power.

Keywords: Discrete gradient; Differential operator; Constitutive equation; Numerical modeling

1. INTRODUCTION

Coming back to 5th century BC, the famous paradox of Achilles and a tortoise regains its significance in numerical models as far as the increasing computational power condenses arrays of treated nodes so that maps of related variables get appearance of continuous fields. At the same time, whatever spacing of nodal points, they remain intractable by the differential operators defined for *infinitesimal* domains. Hence, to directly make use of constitutive differential equations in the numerical modeling, these operators should be properly extended to discrete data. Even though such counterparts of gradient will extract only locally linear parts of underlying continuous fields, in dense enough nodal patterns the neglected non-linear residuals are insignificant.

Meanwhile, instead of the truly discrete approach, artificial functions are commonly presumed to mimic continuous fields between the nodes [1,2]. For instance, a virtual deformation field corresponding to nodal displacements is sought to nullify internal nodal forces as prescribed by the stress balance condition. Let alone inaccuracy of such a priori approximations called shape functions, they lead to computational expenses particularly crucial in case of element-free models [3,4].

Although the latter avoid an awkward remeshing procedure peculiar to specific problems, respective shape functions prove to be overcomplicated [5] and hence hardly suitable for routine applications because of an excessive computational cost. To exclude this drawback of the element-free modeling, the present paper considers discrete extensions of the gradient and related operators applicable immediately to nodal variables. Based on the general algebraic grounds [6,7], these terms are uniquely defined and their use is illustrated on various constitutive equations of solid mechanics.

2. DISCRETE DIFFERENTIAL OPERATORS

Let a cluster of nodal points be specified by $3 \times N$ matrix \mathbf{R} composed of columns which contain Cartesian components of their position vectors \mathbf{r}_j ($j = 1, 2, \dots, N$). To illustrate the discrete differentiation, similar matrix \mathbf{U} made of nodal displacements \mathbf{u}_j is also considered. As shown in [8,9], a pseudoinverse coordinate matrix

$$\mathbf{R}^{-1} = \mathbf{R}^T (\mathbf{R}\mathbf{R}^T)^{-1} \quad (1)$$

of $N \times 3$ dimensions, where determinant of $\mathbf{R}\mathbf{R}^T$ differs from zero and superscript T means transposition, is the

* Corresponding author: A.A. Zisman, e-mail: crism_ru@yahoo.co.uk

unique expression of gradient that has relevant properties. Specifically, the related uniform distortion

$$\mathbf{D} = \nabla \mathbf{u} = (\mathbf{UR}^{-1})^T \quad (2)$$

suggests matrix $\mathbf{U}^* = \mathbf{D}^T \mathbf{R}$ of virtual displacements whose components are most close to those of given \mathbf{U} in terms of the mean square deviation. This proximity corresponds to the Moore-Penrose pseudoinverse [6,7] that takes on a specific form of Eq. (1) when applied to a set of discrete coordinates. However, the considered matrix hides contributions of individual nodes to the gradient or any related operator. To get representation of \mathbf{R}^{-1} in a form more apparent from this viewpoint, we will employ partial gradient vectors as follows.

2.1. Gradient

In the considered cluster of N nodal points each of the latter is specified by individual gradient vector

$$\mathbf{g}_i = \mathbf{r}_i \cdot \left(\sum_{k=1}^N \mathbf{r}_k \otimes \mathbf{r}_k \right)^{-1}, \quad (3)$$

where \mathbf{r}_i are position vectors, dot and \otimes indicate the scalar and tensor products, respectively. According to Ref. [10], this enables a simple expression of the above-mentioned distortion

$$\mathbf{D} = \nabla \mathbf{u} = \sum_{i=1}^N \mathbf{g}_i \otimes \mathbf{u}_i. \quad (4)$$

To exclude irrelevant $\mathbf{D} \neq 0$ in case of the rigid body translation (equal \mathbf{u}_i), the coordinate origin of the cluster is selected so that

$$\sum_{i=1}^N \mathbf{r}_i = 0. \quad (5)$$

A similar formulation of discrete gradient was introduced in Ref. [11] regardless of the pseudoinverse concept; however, this finding remains equivalent to the latter in terms of algebraic properties. Unlike an approach adjusted to lattice-like structures [12], the considered method does not strongly restrict the arrangement of nodal points. Indeed, to ensure existence of an inverse tensor in Eq. (3), only colinear and coplanar patterns are rejected in 2D and 3D modeling, respectively.

The considered discrete differentiation can apply to nodal variables of any type. For example, if scalar potentials φ_i are treated instead of previous displacement vectors, the underlying vector field is expressed by

$$\mathbf{e} = -\nabla \varphi = -\sum_{i=1}^N \mathbf{g}_i \varphi_i. \quad (6)$$

Performance of the present approach has been verified first on the strain mapping of low deformed specimens [13], where movements of nodal points were recorded by the digital image correlation. As to numerical models of solid mechanics, they can avoid continuous approximations insofar as Eq. (4) enables expression of nodal distortions and, hence, strains and stresses *immediately* in terms of nodal displacements.

2.2. Divergence

Replacement of dyads in Eq. (4) by scalar products of involved vectors apparently results in the divergence of displacements

$$\nabla \cdot \mathbf{u} = \sum_{i=1}^N \mathbf{g}_i \cdot \mathbf{u}_i \quad (7)$$

that specifies the local dilatation of deformed matter. Similarly, the stress divergence important in solid mechanics is expressed by

$$\nabla \cdot \boldsymbol{\sigma} = \sum_{i=1}^N \mathbf{g}_i \cdot \boldsymbol{\sigma}_i. \quad (8)$$

It is worth noting that the latter implies *double* differentiation as far as each nodal stress $\boldsymbol{\sigma}_i$ is derived for some sub-cluster of M nodes shifted from the common coordinate origin. To this end, an expression of linear or non-linear elastic response applies to strain

$$\boldsymbol{\varepsilon}_i = \sum_{j=1}^M (\mathbf{g}_j^{(i)} \otimes \mathbf{u}_j + \mathbf{u}_j \otimes \mathbf{g}_j^{(i)}) / 2 \quad (9)$$

that is a symmetric part of distortion according to Eq. (4). For simplicity sake, we will illustrate this approach on 2D models. To quicken calculations and enhance precision of the local stress divergence by diminishing differentiation domains, computations are implemented as follows.

First, related to nodal displacement (Fig. 1a), virtual strains $\boldsymbol{\varepsilon}_i$ are derived with Eq. (9) for the triple sub-clusters ($M = 3$) shown in Fig. 1b; next, to calculate the stress divergence, respective stresses $\boldsymbol{\sigma}_i$ are ascribed to provisional nodal points symmetrically situated on virtual border lines connecting the permanent nodes as illustrated in Fig. 1c. Thus, if \mathbf{i} and \mathbf{j} are directions of axes X and Y , respectively, partial gradient vectors expressed by Eq. (3) with $N = 4$ take on form

$$\begin{aligned} \mathbf{g}_1 &= b^{-1}(\mathbf{i} + \mathbf{j})/2, & \mathbf{g}_2 &= b^{-1}(-\mathbf{i} + \mathbf{j})/2, \\ \mathbf{g}_3 &= -b^{-1}(\mathbf{i} + \mathbf{j})/2, & \mathbf{g}_4 &= b^{-1}(\mathbf{i} - \mathbf{j})/2. \end{aligned} \quad (10)$$

In this case Eq. (8) results in

$$\nabla \cdot \boldsymbol{\sigma} = b^{-1} \{ \mathbf{i} \cdot (\boldsymbol{\sigma}_1 + \boldsymbol{\sigma}_4 - \boldsymbol{\sigma}_2 - \boldsymbol{\sigma}_3) + \mathbf{j} \cdot (\boldsymbol{\sigma}_1 + \boldsymbol{\sigma}_2 - \boldsymbol{\sigma}_3 - \boldsymbol{\sigma}_4) \} / 2. \quad (11)$$

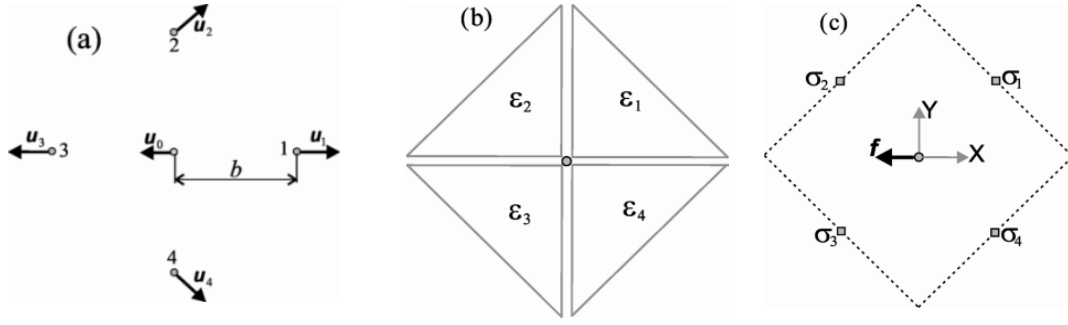


Fig. 1. Treated variables: (a) nodal displacements and (b) related strains of triangle sub-clusters; (c) virtual locations of corresponding stresses to derive a nodal force at the cluster center in terms of stress divergence.

Therefore, with Eq. (8) kept in mind, the nodal force per unit thickness can be evaluated by

$$\mathbf{f} = -b^2 \sum_{j=1}^N \mathbf{g}_j \cdot \boldsymbol{\sigma}_j \quad (12)$$

that is a discrete extension of the conventional stress balance equation.

2.3. Rotor

The discrete rotor in terms of partial gradient vectors can apply to vector or tensor variables. Thus, when applied to nodal displacements, it results in the rotation vector

$$\mathbf{w} = \nabla \times \mathbf{u} / 2 = \left(\sum_{i=1}^N \mathbf{g}_i \times \mathbf{u}_i \right) / 2 \quad (13)$$

corresponding to the skew part of distortion. If field \mathbf{D} of the nodal *elastic* distortions is known, the dislocation density tensor

$$\boldsymbol{\alpha} = \nabla \times \mathbf{D} = \sum_{i=1}^N \mathbf{g}_i \times \mathbf{D}_i \quad (14)$$

is expressed, extending the continual theory of defects [14]. One can make use of this expedient since up-to-date techniques of electron microscopy enable measurements of \mathbf{D}_i at separated points of a planar section [15]. Besides, when applied twice, the same operator extends to nodal variables the known Saint-Venant condition of strain compatibility:

$$\nabla \times \boldsymbol{\varepsilon} \times \nabla = \sum_{i=1}^N \sum_{j=1}^M \mathbf{g}_i \times (\boldsymbol{\varepsilon}_j^{(i)} \times \mathbf{g}_j^{(i)}) = 0. \quad (15)$$

Similar to Eqs. (8) and (9), respectively, N and M in this expression number auxiliary sub-clusters and nodal points in each of the latter. The middle part of Eq. (15) is also applicable in numerical modeling of internal stresses. Indeed, when nodal strains are elastic, a deviation of this term from zero is the discrete counterpart of strain *incompatibility* tensor [16] specifying strength of a stress source (defect).

2.4. Laplasian and gradient of divergence

Based on partial gradient vectors, Laplasian of any field \mathbf{F} is also expressed in terms of nodal variables:

$$\Delta \mathbf{F} = \nabla \cdot \nabla \mathbf{F} = \sum_{i=1}^N \sum_{j=1}^M \mathbf{g}_i \cdot \mathbf{g}_j^{(i)} \mathbf{F}_j^{(i)}. \quad (16)$$

In solid mechanics, for example, nodal stress *tensors* $\boldsymbol{\sigma}_j^{(i)}$ should be taken for $\mathbf{F}_j^{(i)}$ to extend the constitutive Beltrami-Michell equation. Alternatively, to make use of Lamé's equation, the Laplasian of displacements should be derived from nodal *vectors* $\mathbf{u}_j^{(i)}$. The gradient of divergence is another related operator needed in this special case and some other applications. Within the present formulation the desired term takes on form

$$\nabla \nabla \cdot \mathbf{u} = \sum_{i=1}^N \sum_{j=1}^M \mathbf{g}_i (\mathbf{g}_j^{(i)} \cdot \mathbf{u}_j^{(i)}). \quad (17)$$

3. SOME EXAMPLES

To illustrate use of nodal gradient vectors, principal in this paper, let us consider first a square cluster undergoing two opposite nodal displacements ($\mathbf{u}_2 = -\mathbf{u}_1 = 2u\mathbf{i}$) as shown in Fig. 2a. In this case Eq. (4) with gradient vectors related to the four corners results in virtually uniform simple shear

$$\mathbf{D} = (2u/b) \mathbf{j} \otimes \mathbf{i}, \quad (18)$$

that suggests displacements (Fig. 2b)

$$\mathbf{u}_2^* = \mathbf{u}_3^* = -\mathbf{u}_1^* = u\mathbf{i}. \quad (19)$$

The latter notably differ from *given* \mathbf{u}_1 and \mathbf{u}_2 , but provide the same uniform distortion when substituted in Eq. (4). In other words, fractions $\boldsymbol{\delta}_i = \mathbf{u}_i - \mathbf{u}_i^*$ of \mathbf{u}_i ($i = 1, 2, 3, 4$) render no effect on the gradient operation and prove to be in a sense excessive. This result illustrated in Fig. 2c supports the present formulation as far as such fractions are due to essentially inhomogeneous distortions averaging out to zero and hence irrelevant to the sought distortion of the *whole* cluster.

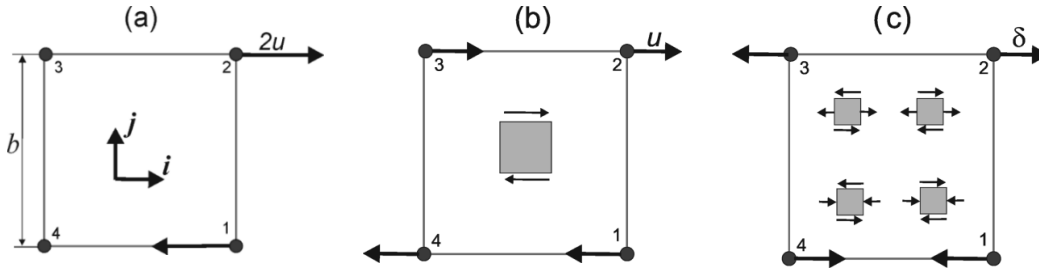


Fig. 2. Deformed trial cluster: (a) applied nodal displacements, (b) their constituents due to the uniform part of distortion, and (c) the residuals filtered out in discrete differentiation over the whole cluster.

Next, applicability of the discrete stress balance equation (Subsection 2.2) to discrete models of solid mechanics deserves consideration. For instance, this equation enables determination of local stiffness terms while avoiding predefined shape functions. Indeed, to determine the force-to-displacement ratios, Eq. (12) can express nodal forces due to trial nodal displacements. Apart from the numerical modeling of continuum represented by a set of virtual nodal points, the considered formulation becomes most natural when applied to physically discrete structures such as cores of crystal defects. For instance, a short-range disorder introducing the Burgers vector of an edge dislocation in a virtual initial configuration (Fig. 3a) violates the stress balance between neighboring atoms. Thus, according to Ref. [10], in the crystal that has a finite cross section containing 10050 atoms the maximum magnitude of f reaches $Gb/2$, where G is the shear modulus. To approach the balance ($f=0$ at each atom) with a stated tolerance, corrective displacements proportional to fictitious forces expressed by Eq. (12) should be repeatedly applied. Fig. 3b compiled from Ref. [10] illustrates the relaxed state where such forces have been reduced by three orders. A remark should be made that

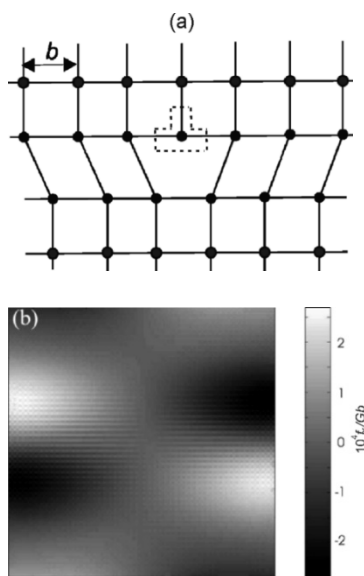


Fig. 3. Dislocated crystal: (a) a representative part of the virtual initial configuration, (b) residual fictitious forces in the *relaxed* crystal over its finite section (10050 atoms).

these results are due to isotropic non-linear elasticity expressed in terms of theoretical crystal strength (TCS) to allow for specific stiffness on the core scale.

Corresponding to the above-mentioned relaxation degree, Fig. 4 shows a final shape of the crystal where short-range stresses at the dislocation core prove to comply with the TCS and predicted core dimensions are very close to relevant data of high-resolution electron microscopy [17].

4. SPECIAL PROPERTIES OF PERIODICAL NODAL PATTERN

Usage of atom positions for nodal points is indispensable in application of the present formulation to crystalline structures. On the one hand, periodical patterns ensure the natural symmetry of crystal properties [12]; on the other hand, this approach explicitly reflects the short-range disorder at microscopic cores of lattice defects. At the same

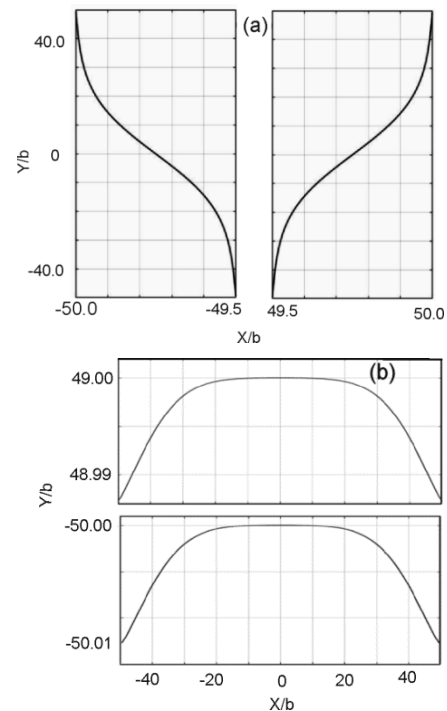


Fig. 4. Appearance of the lateral (a) and initially horizontal (b) crystal borders due to insertion of an edge dislocation according to Fig. 3a and the following relaxation.

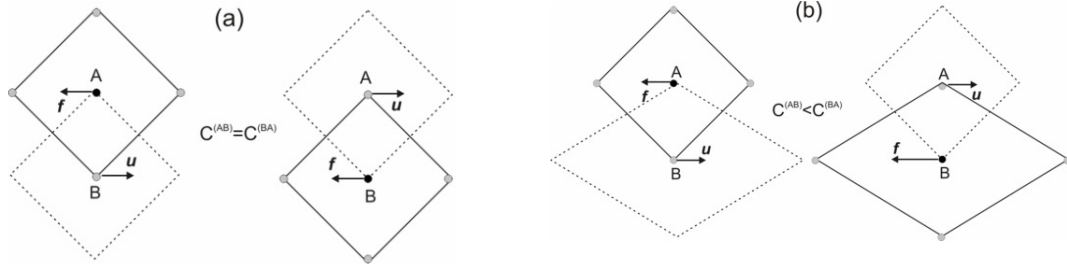


Fig. 5. Interaction of neighboring nodes: (a) symmetry of stiffness in case of uniform discretization, and (b) violation of the symmetry otherwise.

time, if a discrete model mimics some continuous matter, the arrangement of separated nodes deserves a special discussion as follows.

Since the present paper focuses on solid mechanics, it is relevant to revisit the nodal stiffness issue. Conventional stiffness coefficients in expression

$$f_m = C_{mn} u_n \quad (20)$$

of nodal forces in terms of nodal displacements should be symmetric insofar as

$$C_{mn} = -\frac{\partial^2 W}{\partial u_n \partial u_m} = -\frac{\partial^2 W}{\partial u_m \partial u_n} = C_{nm}, \quad (21)$$

where W is elastic energy. Natural m and n in these equations simultaneously number both the considered points and Cartesian components of related variables; in case of 2D model with K nodes, $m, n = 1, 2, \dots, 2K$ and any $m = n$ corresponds to similar components of force and displacement at the same point. Unlike the total numeration in Eqs. (20) and (21), it is advisable to make use of *local* denotations (Fig. 1a) facilitating analysis. Thus, with the central node numbered by zero, stiffness components

$$\begin{aligned} C_{xx}^{(00)} &= \frac{f_x^{(0)}}{u_x^{(0)}}, & C_{xy}^{(00)} &= \frac{f_x^{(0)}}{u_y^{(0)}}, & C_{yx}^{(00)} &= \frac{f_y^{(0)}}{u_x^{(0)}}, & C_{yy}^{(00)} &= \frac{f_y^{(0)}}{u_y^{(0)}}, \\ C_{xx}^{(01)} &= \frac{f_x^{(0)}}{u_x^{(1)}}, & C_{xy}^{(01)} &= \frac{f_x^{(0)}}{u_y^{(1)}}, & C_{xx}^{(02)} &= \frac{f_x^{(0)}}{u_x^{(2)}}, & \dots, & C_{yy}^{(04)} &= \frac{f_y^{(0)}}{u_y^{(4)}} \end{aligned} \quad (22)$$

are readily expressed in terms of trial nodal displacements and resulting forces. As illustrated by Fig. 5a, the desired symmetry in interaction of *different* nodes ($f_A(u_B)$ and $f_B(u_A)$ at $r_A \neq r_B$) is ensured only if they have similar surroundings, i.e., the whole pattern has translational symmetry; otherwise (Fig. 5b), two dissimilar clusters different in their discrete gradients would suggest $C_{xx}^{(AB)} \neq C_{xx}^{(BA)}$. Periodical patterns also keep Eq. (21) valid for any *single* node A ; indeed, $C_{xy}^{(AA)} = C_{yx}^{(AA)} = 0$ since all its neighbors are situated symmetrically relative to directions x and y .

Periodicity of discrete models physically prescribed by Eq. (21) leads to both advantages and difficulties. This requirement facilitates the modeling as far as all C_{mn} can be predetermined on a unique arrangement of neighboring nodes. Moreover, since $f \sim b^2 g \sigma$ with $g \sim 1/b$ and $\sigma \sim G \varepsilon \sim Gu/b$ in Eq. (12), force-to-displacement ratios do not depend on b and, hence, the same stiffness terms will be valid for whatever periodical pattern condensed to treat singular fields. At the same time, to *separately* simulate related local domains, specific boundary conditions should be somehow derived from the periodical pattern uniform over the whole model.

Appropriate procedures to resolve the indicated problem would in a sense resemble element-free inclusions in FEM models [18] and singular enrichment functions on the background of a uniform FEM mesh [19]. Even though the considered approach suggests some complications, it will be hardly inferior to the usually gradual refinement of discretization when approaching stress singularities. Indeed, the latter method still remains intuitive and does not ensure the best compromise between accuracy and computational efficiency. Besides, the violation of stiffness symmetry in case of non-periodical discrete patterns (Fig. 5b) suggests the *artificial* non-uniformity of elastic properties over the simulated continuous matter.

5. CONCLUDING REMARKS

The conventional gradient and related differential operators have been uniquely extended to nodal variables regardless of uncertain fields between the nodal points. Whichever phenomena are simulated, these findings provide proper discrete counterparts of governing differential equations directly applicable in the numerical modeling. When special constraints (e.g., symmetry of stiffness) do matter, periodical nodal patterns are indispensable which suggest both limitations and advantages. At the same time, whatever discrete pattern is suitable if the problem is essentially geometrical (computer graphics, strain mapping, etc.).

A remark should be made as well that various gradient theories (see, e.g., Refs. [19,20]) have been developed to implicitly reflect *discrete* constitution of real solids within

the framework of *continuum* mechanics. It would be interesting to verify their specific parameters by the proposed method that can directly treat in mechanistic terms the interaction of atoms in crystalline matter.

REFERENCES

- [1] O.C. Zienkiewicz, *The finite element method: from intuition to generality*, Appl. Mech. Rev., 1970, vol. 23, pp. 249–256.
- [2] R.H. Gallager, *Finite element analysis*, Prentice-Hall, New Jersey, 1975.
- [3] T. Belytschko, Y. Krongauz, D. Organ, M. Fleming, P. Krysl, *Meshless methods: an overview and recent developments*, Comp. Meth. Appl. Mech. Eng., 1996, vol. 139, no. 1–4, pp. 3–47.
- [4] Y. Chen, J. Lee, A. Eskandarian, *Meshless methods in solid mechanics*, Springer, New York, 2006.
- [5] X. Pan, K.Y. Sze, X. Zhang, *An assessment of the meshless weighted least-square method*, Acta Mech. Solida Sin., 2004, vol. 17, no. 3, pp. 270–282.
- [6] E.H. Moore, *On the reciprocal of the general algebraic matrix*, Bull. Amer. Math. Soc., 1920, vol. 26, pp. 394–395.
- [7] R. Penrose, *A generalized inverse for matrices*, Proc. Camb. Philos. Soc., 1955, vol. 51, no. 3, pp. 406–413.
- [8] A. Zisman, N. Ermakova, *Deformation and stiffness of finite element with no assumed interpolation for bulk velocity field*, J. Mech. Behav. Mater., 2006, vol. 17, no. 4, pp. 219–234.
- [9] A. Zisman, *Interpolation-free discrete modeling with gradient matrix: Case study of edge dislocation in linearly elastic crystal*, Int. J. Eng. Sci., 2014, vol. 78, pp. 124–133.
- [10] A.A. Zisman, N.Y. Ermakova, *Elastically non-linear discrete model for core of edge dislocation*, Int. J. Eng. Sci., 2022, vol. 174, art. no. 103670.
- [11] M.F. Horstemeyer, M.I. Baskes, *Strain tensor at the atomic scale*, MRS Online Proc. Library, 1999, vol. 578, pp. 15–20.
- [12] M.R. Banerjee, R. Ramadugu, S. Ansumali, *Discrete differential operators on a class of lattices*, J. Comp. Sci., 2020, vol. 44, art. no. 101172.
- [13] A.A. Zisman, D.S. Ivanov, S.V. Lomov, I. Verpoest, *Processing discrete data by gradient matrix: Application to strain mapping of textile composite*, in: Proc. 12th Eur. Conf. Compos. Mater. (CD ROM), ed. by J. Lamon, A.T. Marques, Biarritz, 2006.
- [14] J.P. Hirth, J. Lothe, *Theory of dislocations*, McGraw-Hill, New York, 1968.
- [15] A.J. Wilkinson, G. Meaden, D.J. Dingley, *High-resolution elastic strain measurement from electron backscatter diffraction patterns: New levels of sensitivity*, Ultramicroscopy, 2006, vol. 106, no. 4–5, pp. 307–313.
- [16] E. Kröner, *Kontinuumstheorie der versetzungen und eigenspannungen*. Springer Verlag, Berlin, 1958.
- [17] C.W. Zhao, Y.M. Xing, C.E. Zhou, P.C. Bai, *Experimental examination of displacement and strain fields in an edge dislocation core*, Acta Mater., 2008, vol. 56, no. 11, pp. 2570–2575.
- [18] H. Karutz, R. Chudoba, W.B. Krätzig, *Automatic adaptive generation of a coupled finite element/element-free Galerkin discretization*, Finite Elem. Anal. Des., 2002, vol. 38, no. 11, pp. 1075–1091.
- [19] T. Belytschko, R. Gracie, G. Ventura, *A review of extended/generalized finite element methods for material modeling*, Model. Simul. Mater. Sci. Eng., 2009, vol. 17, no. 4, art. no. 043001.
- [20] R.D. Mindlin, *Second gradient of strain and surface-tension in linear elasticity*, Int. J. Solids Struct., 1965, vol. 1, no. 4, pp. 417–438.
- [21] E.C. Aifantis, *A concise review of gradient models in mechanics and physics*, Front. Phys., 2020, vol. 7, art. no. 239.

УДК 539.3

Применение дискретных дифференциальных операторов в численных моделях механики твердого тела

А.А. Зисман, Н.Ю. Ермакова

Физико-механический институт, Санкт-Петербургский политехнический университет Петра Великого,
Политехническая ул., д. 29, Санкт-Петербург, 195251, Россия

Аннотация. В статье представлены результаты применения градиента и связанных с ним дифференциальных операторов к массиву узловых точек сплошной среды. Этот подход позволяет избежать введения искусственных функций формы для представления определяющих соотношений в моделях механики твердого тела. Численное моделирование может быть выполнено непосредственно в терминах узловых переменных. Точность моделирования возрастает при уменьшении расстояния между узлами, однако требует дополнительных вычислительных мощностей.

Ключевые слова: дискретный градиент; дифференциальный оператор; определяющие соотношения; численное моделирование